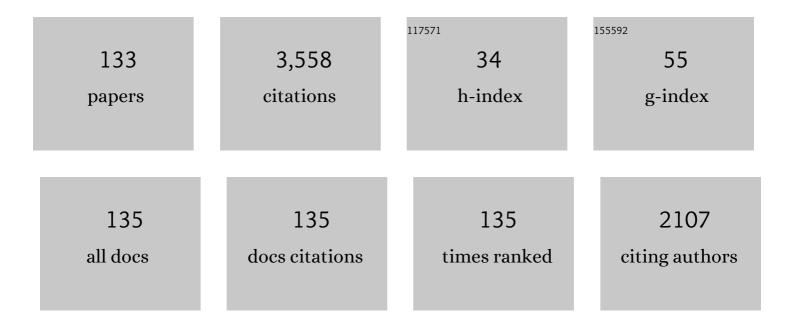
List of Publications by Year in descending order

Source: https://exaly.com/author-pdf/1211626/publications.pdf Version: 2024-02-01



STEDHEN S CAO

#	Article	IF	CITATIONS
1	Temporal variation of seismicb-values beneath northeastern Japan island arc. Geophysical Research Letters, 2002, 29, 48-1-48-3.	1.5	190
2	SKSsplitting beneath continental rift zones. Journal of Geophysical Research, 1997, 102, 22781-22797.	3.3	143
3	Southern African crustal evolution and composition: Constraints from receiver function studies. Journal of Geophysical Research, 2006, 111, n/a-n/a.	3.3	141
4	Seismic anisotropy and mantle flow beneath the Baikal rift zone. Nature, 1994, 371, 149-151.	13.7	116
5	Mantle deformation beneath southern Africa. Geophysical Research Letters, 2001, 28, 2493-2496.	1.5	115
6	Deep structure and origin of the Baikal rift zone. Earth and Planetary Science Letters, 2006, 243, 681-691.	1.8	102
7	Determining crustal structure beneath seismic stations overlying a lowâ€velocity sedimentary layer using receiver functions. Journal of Geophysical Research: Solid Earth, 2015, 120, 3208-3218.	1.4	96
8	Shear wave splitting and mantle flow associated with the deflected Pacific slab beneath northeast Asia. Journal of Geophysical Research, 2008, 113, .	3.3	91
9	Mantle transition zone discontinuities beneath the contiguous United States. Journal of Geophysical Research: Solid Earth, 2014, 119, 6452-6468.	1.4	83
10	Upper mantle structure of the Saharan Metacraton. Journal of African Earth Sciences, 2011, 60, 328-336.	0.9	81
11	Northridge Earthquake Damage Caused by Geologic Focusing of Seismic Waves. Science, 2000, 289, 1746-1750.	6.0	76
12	Low seismic velocity layers in the Earth's crust beneath Eastern Siberia (Russia) and Central Mongolia: receiver function data and their possible geological implication. Tectonophysics, 2002, 359, 307-327.	0.9	75
13	Asymmetric upwarp of the asthenosphere beneath the Baikal rift zone, Siberia. Journal of Geophysical Research, 1994, 99, 15319.	3.3	73
14	Crustal anisotropy and ductile flow beneath the eastern Tibetan Plateau and adjacent areas. Earth and Planetary Science Letters, 2016, 442, 72-79.	1.8	72
15	Annual modulation of triggered seismicity following the 1992 Landers earthquake in California. Nature, 2000, 406, 500-504.	13.7	66
16	Seismic anisotropy beneath the Afar Depression and adjacent areas: Implications for mantle flow. Journal of Geophysical Research, 2010, 115, .	3.3	66
17	Seismic anisotropy, mantle fabric, and the magmatic evolution of Precambrian southern Africa. South African Journal of Geology, 2004, 107, 45-58.	0.6	65
18	Making Reliable Shear-Wave Splitting Measurements. Bulletin of the Seismological Society of America, 2013, 103, 2680-2693.	1.1	64

#	Article	IF	CITATIONS
19	Evidence for small-scale mantle convection in the upper mantle beneath the Baikal rift zone. Journal of Geophysical Research, 2003, 108, .	3.3	59
20	Spatial variation of seismic b-values beneath Makushin Volcano, Unalaska Island, Alaska. Earth and Planetary Science Letters, 2006, 245, 408-415.	1.8	59
21	Mantle discontinuities beneath Southern Africa. Geophysical Research Letters, 2002, 29, 129-1-129-4.	1.5	56
22	Mantle layering across central South America. Journal of Geophysical Research, 2003, 108, .	3.3	54
23	Significant seismic anisotropy beneath the southern Lhasa Terrane, Tibetan Plateau. Geochemistry, Geophysics, Geosystems, 2009, 10, .	1.0	53
24	Spatial variations of crustal characteristics beneath the Hoggar swell, Algeria, revealed by systematic analyses of receiver functions from a single seismic station. Geochemistry, Geophysics, Geosystems, 2010, 11, .	1.0	53
25	Magnetic stripes of a transitional continental rift in Afar. Geology, 2012, 40, 203-206.	2.0	47
26	Complex seismic anisotropy beneath western Tibet and its geodynamic implications. Earth and Planetary Science Letters, 2015, 413, 167-175.	1.8	47
27	A uniform database of teleseismic shear wave splitting measurements for the western and central United States. Geochemistry, Geophysics, Geosystems, 2014, 15, 2075-2085.	1.0	46
28	Significant crustal thinning beneath the Baikal rift zone: New constraints from receiver function analysis. Geophysical Research Letters, 2004, 31, .	1.5	45
29	SKS splitting beneath southern California. Geophysical Research Letters, 1995, 22, 767-770.	1.5	43
30	Seismic azimuthal anisotropy beneath the eastern United States and its geodynamic implications. Geophysical Research Letters, 2017, 44, 2670-2678.	1.5	43
31	Formation of the Cameroon Volcanic Line by lithospheric basal erosion: Insight from mantle seismic anisotropy. Journal of African Earth Sciences, 2014, 100, 96-108.	0.9	42
32	Receiver function constraints on crustal seismic velocities and partial melting beneath the Red Sea rift and adjacent regions, Afar Depression. Journal of Geophysical Research: Solid Earth, 2014, 119, 2138-2152.	1.4	41
33	Imaging mantle discontinuities using multiply-reflected P-to-S conversions. Earth and Planetary Science Letters, 2014, 402, 99-106.	1.8	40
34	Analysis of deformation data at Parkfield, California: Detection of a long-term strain transient. Journal of Geophysical Research, 2000, 105, 2955-2967.	3.3	38
35	Crustal Azimuthal Anisotropy Beneath the Southeastern Tibetan Plateau and its Geodynamic Implications. Journal of Geophysical Research: Solid Earth, 2018, 123, 9733-9749.	1.4	36
36	Lithospheric layering beneath the contiguous United States constrained by S-to-P receiver functions. Earth and Planetary Science Letters, 2018, 495, 79-86.	1.8	35

#	Article	IF	CITATIONS
37	Mantle flow and lithosphere–asthenosphere coupling beneath the southwestern edge of the North American craton: Constraints from shear-wave splitting measurements. Earth and Planetary Science Letters, 2014, 402, 209-220.	1.8	34
38	Mantle transition zone discontinuities beneath the Indochina Peninsula: Implications for slab subduction and mantle upwelling. Geophysical Research Letters, 2017, 44, 7159-7167.	1.5	33
39	Apparent Weekly and Daily Earthquake Periodicities in the Western United States. Bulletin of the Seismological Society of America, 2009, 99, 2273-2279.	1.1	32
40	Crustal structure and evolution beneath the Colorado Plateau and the southern Basin and Range Province: Results from receiver function and gravity studies. Geochemistry, Geophysics, Geosystems, 2011, 12, n/a-n/a.	1.0	32
41	Estimation of the Depth of Anisotropy Using Spatial Coherency of Shear-Wave Splitting Parameters. Bulletin of the Seismological Society of America, 2011, 101, 2153-2161.	1.1	31
42	Seismic anisotropy and mantle flow beneath the northern Great Plains of North America. Journal of Geophysical Research: Solid Earth, 2014, 119, 1971-1985.	1.4	31
43	Mantle transition zone discontinuities beneath the Baikal rift and adjacent areas. Journal of Geophysical Research, 2006, 111, n/a-n/a.	3.3	28
44	Azimuthal anisotropy and mantle flow underneath the southeastern Tibetan Plateau and northern Indochina Peninsula revealed by shear wave splitting analyses. Tectonophysics, 2018, 747-748, 68-78.	0.9	28
45	AnisDep: A FORTRAN program for the estimation of the depth of anisotropy using spatial coherency of shear-wave splitting parameters. Computers and Geosciences, 2012, 49, 330-333.	2.0	27
46	A joint receiver function and gravity study of crustal structure beneath the incipient Okavango Rift, Botswana. Geophysical Research Letters, 2015, 42, 8398-8405.	1.5	26
47	Seismic anisotropy beneath the incipient Okavango rift: Implications for rifting initiation. Earth and Planetary Science Letters, 2015, 430, 1-8.	1.8	26
48	Seismic anisotropy of the uppermost mantle beneath the Rio Grande rift: Evidence from Kilbourne Hole peridotite xenoliths, New Mexico. Earth and Planetary Science Letters, 2011, 311, 172-181.	1.8	24
49	Seismic Arrays to Study African Rift Initiation. Eos, 2013, 94, 213-214.	0.1	23
50	No thermal anomalies in the mantle transition zone beneath an incipient continental rift: evidence from the first receiver function study across the Okavango Rift Zone, Botswana. Geophysical Journal International, 2015, 202, 1407-1418.	1.0	23
51	Shear wave splitting analyses in Tian Shan: Geodynamic implications of complex seismic anisotropy. Geochemistry, Geophysics, Geosystems, 2016, 17, 1975-1989.	1.0	21
52	Evolution of the broadly rifted zone in southern Ethiopia through gravitational collapse and extension of dynamic topography. Tectonophysics, 2017, 699, 213-226.	0.9	21
53	Crustal structure beneath the Malawi and Luangwa Rift Zones and adjacent areas from ambient noise tomography. Gondwana Research, 2019, 67, 187-198.	3.0	21
54	Characteristics of mantle fabrics beneath the south-central United States: Constraints from shear-wave splitting measurements. , 2008, 4, 411.		20

#	Article	lF	CITATIONS
55	A Uniform Database of Teleseismic Shearâ€Wave Splitting Measurements for the Western and Central United States: December 2014 Update. Seismological Research Letters, 2016, 87, 295-300.	0.8	20
56	Toroidal Mantle Flow Induced by Slab Subduction and Rollback Beneath the Eastern Himalayan Syntaxis and Adjacent Areas. Geophysical Research Letters, 2019, 46, 11080-11090.	1.5	20
57	Seismic imaging of mantle transition zone discontinuities beneath the northern Red Sea and adjacent areas. Geophysical Journal International, 2014, 199, 648-657.	1.0	19
58	Passive rifting of thick lithosphere in the southern East African Rift: Evidence from mantle transition zone discontinuity topography. Journal of Geophysical Research: Solid Earth, 2016, 121, 8068-8079.	1.4	19
59	Topography of the Mantle Transition Zone Discontinuities Beneath Alaska and Its Geodynamic Implications: Constraints From Receiver Function Stacking. Journal of Geophysical Research: Solid Earth, 2017, 122, 10,352.	1.4	19
60	Seismic anisotropy and subduction-induced mantle fabrics beneath the Arabian and Nubian Plates adjacent to the Red Sea. Geophysical Research Letters, 2014, 41, 2376-2381.	1.5	18
61	Seismic anisotropy and mantle dynamics beneath the Malawi Rift Zone, East Africa. Tectonics, 2017, 36, 1338-1351.	1.3	18
62	Mantle structure beneath the incipient Okavango rift zone in southern Africa. , 2017, 13, 102-111.		18
63	Upper mantle and mantle transition zone thermal and water content anomalies beneath NE Asia: Constraints from receiver function imaging of the 410 and 660 km discontinuities. Earth and Planetary Science Letters, 2020, 532, 116040.	1.8	18
64	The mantle transition zone beneath the Afar Depression and adjacent regions: implications for mantle plumes and hydration. Geophysical Journal International, 2016, 205, 1756-1766.	1.0	16
65	Receiver function and gravity constraints on crustal structure and vertical movements of the Upper Mississippi Embayment and Ozark Uplift. Journal of Geophysical Research: Solid Earth, 2017, 122, 4572-4583.	1.4	16
66	Crustal Azimuthal Anisotropy Beneath the Central North China Craton Revealed by Receiver Functions. Geochemistry, Geophysics, Geosystems, 2019, 20, 2235-2251.	1.0	16
67	Seismic Anisotropy and Mantle Flow in the Sumatra Subduction Zone Constrained by Shear Wave Splitting and Receiver Function Analyses. Geochemistry, Geophysics, Geosystems, 2020, 21, e2019GC008766.	1.0	16
68	Characteristics of the Mantle Flow System Beneath the Indochina Peninsula Revealed by Teleseismic Shear Wave Splitting Analysis. Geochemistry, Geophysics, Geosystems, 2018, 19, 1519-1532.	1.0	15
69	Receiver function investigation of crustal structure in the Malawi and Luangwa rift zones and adjacent areas. Gondwana Research, 2021, 89, 168-176.	3.0	14
70	Crustal thickness and Moho sharpness beneath the Midcontinent rift from receiver functions. Research in Geophysics, 2013, 3, 1.	0.7	13
71	Absence of thermal influence from the African Superswell and cratonic keels on the mantle transition zone beneath southern Africa: Evidence from receiver function imaging. Earth and Planetary Science Letters, 2018, 503, 108-117.	1.8	13
72	Slab Dehydration and Mantle Upwelling in the Vicinity of the Sumatra Subduction Zone: Evidence from Receiver Function Imaging of Mantle Transition Zone Discontinuities. Journal of Geophysical Research: Solid Earth, 2020, 125, e2020JB019381.	1.4	13

STEPHEN S GAO

#	Article	IF	CITATIONS
73	Crustal azimuthal anisotropy and deformation beneath the northeastern Tibetan Plateau and adjacent areas: Insights from receiver function analysis. Tectonophysics, 2021, 816, 229014.	0.9	12
74	Lateral variations of crustal structure beneath the Indochina Peninsula. Tectonophysics, 2017, 712-713, 193-199.	0.9	11
75	Mantle Structure and Flow Beneath an Early‣tage Continental Rift: Constraints From <i>P</i> Wave Anisotropic Tomography. Tectonics, 2020, 39, e2019TC005590.	1.3	11
76	Crustal structure beneath the Ethiopian Plateau and adjacent areas from receiver functions: Implications for partial melting and magmatic underplating. Tectonophysics, 2021, 809, 228857.	0.9	11
77	Low-coherent WDM reflectometry for accurate fiber length monitoring. IEEE Photonics Technology Letters, 2003, 15, 96-98.	1.3	10
78	Azimuthal anisotropy beneath north central Africa from shear wave splitting analyses. Geochemistry, Geophysics, Geosystems, 2015, 16, 1105-1114.	1.0	10
79	Foundered lithospheric segments dropped into the mantle transition zone beneath southern California, USA. Geology, 2020, 48, 200-204.	2.0	10
80	Applicability of the Multiple-Event Stacking Technique for Shear-Wave Splitting Analysis. Bulletin of the Seismological Society of America, 2015, 105, 3156-3166.	1.1	9
81	A Systematic Comparison of the Transverse Energy Minimization and Splitting Intensity Techniques for Measuring Shearâ€Wave Splitting Parameters. Bulletin of the Seismological Society of America, 2015, 105, 230-239.	1.1	9
82	Receiver Function Imaging of Mantle Transition Zone Discontinuities Beneath the Tanzania Craton and Adjacent Segments of the East African Rift System. Geophysical Research Letters, 2017, 44, 12,116.	1.5	9
83	Seismic Anisotropy and Mantle Flow Constrained by Shear Wave Splitting in Central Myanmar. Journal of Geophysical Research: Solid Earth, 2021, 126, e2021JB022144.	1.4	9
84	A Database of Shearâ€Wave Splitting Measurements for the Arabian Plate. Seismological Research Letters, 2018, 89, 2294-2298.	0.8	8
85	Reply [to "Comment on "SKS splitting beneath continental rifts zones―by Gao et al.â€]. Journal of Geophysical Research, 1999, 104, 10791-10794.	3.3	7
86	A systematic investigation of piercing-point-dependent seismic azimuthal anisotropy. Geophysical Journal International, 2021, 227, 1496-1511.	1.0	7
87	Potassic Volcanism Induced by Mantle Upwelling Through a Slab Window: Evidence From Shear Wave Splitting Analyses in Central Java. Journal of Geophysical Research: Solid Earth, 2022, 127, .	1.4	7
88	Mantle Flow in the Vicinity of the Eastern Edge of the Pacific‥akutat Slab: Constraints From Shear Wave Splitting Analyses. Journal of Geophysical Research: Solid Earth, 2021, 126, e2021JB022354.	1.4	6
89	Seismic Anisotropy and Mantle Deformation Beneath the Central Sunda Plate. Journal of Geophysical Research: Solid Earth, 2021, 126, e2020JB021259.	1.4	6
90	Lithospheric Structure and Evolution of Southern Africa: Constraints From Joint Inversion of Rayleigh Wave Dispersion and Receiver Functions. Geochemistry, Geophysics, Geosystems, 2019, 20, 3311-3327.	1.0	5

#	Article	IF	CITATIONS
91	Spatial Variations of Upper Crustal Anisotropy Along the San Jacinto Fault Zone in Southern California: Constraints From Shear Wave Splitting Analysis. Journal of Geophysical Research: Solid Earth, 2021, 126, e2020JB020876.	1.4	5
92	Crustal structure and subsidence mechanisms of the Williston Basin: New constraints from receiver function imaging. Earth and Planetary Science Letters, 2022, 593, 117686.	1.8	5
93	Receiver function imaging of the 410 and 660Âkm discontinuities beneath the Australian continent. Geophysical Journal International, 2020, 220, 1481-1490.	1.0	4
94	Crustal modifications beneath the central Sunda plate associated with the Indo-Australian subduction and the evolution of the South China Sea. Physics of the Earth and Planetary Interiors, 2020, 306, 106539.	0.7	4
95	Layered mantle heterogeneities associated with post-subducted slab segments. Earth and Planetary Science Letters, 2021, 571, 117115.	1.8	4
96	Stagnation and tearing of the subducting northwest Pacific slab. Geology, 2022, 50, 676-680.	2.0	4
97	Classification of Teleseismic Shear Wave Splitting Measurements: A Convolutional Neural Network Approach. Geophysical Research Letters, 2022, 49, .	1.5	4
98	Integrated geologic, geophysical, and petrophysical data to construct full field geologic model of Cambrian-Ordovician and Upper Cretaceous reservoir formations, Central Western Sirte Basin, Libya. Interpretation, 2019, 7, T21-T37.	0.5	3
99	Topography of the 410 and 660Âkm Discontinuities Beneath the Cenozoic Okavango Rift Zone and Adjacent Precambrian Provinces. Journal of Geophysical Research: Solid Earth, 2020, 125, e2019JB019290.	1.4	3
100	Crustal P-wave velocity structure and earthquake distribution in the Jiaodong Peninsula, China. Tectonophysics, 2021, 814, 228973.	0.9	3
101	Continental Breakâ€Up Under a Convergent Setting: Insights From P Wave Radial Anisotropy Tomography of the Woodlark Rift in Papua New Guinea. Geophysical Research Letters, 2022, 49, .	1.5	3
102	Characterization of a Continuous, Very Narrowband Seismic Signal near 2.08 Hz. Bulletin of the Seismological Society of America, 2001, 91, 1910-1916.	1.1	2
103	A full field static model of the RG-oil field, central Sirte Basin, Libya. , 2016, , .		2
104	Fault visualization enhancement using ant tracking technique and its application in the Taranaki basin, new Zealand. , 2017, , .		2
105	Receiver Function Investigations of Seismic Anisotropy Layering Beneath Southern California. Journal of Geophysical Research: Solid Earth, 2018, 123, 10,672.	1.4	2
106	Teleseismic <i>P</i> â€Wave Attenuation Beneath the Southeastern United States. Geochemistry, Geophysics, Geosystems, 2021, 22, e2021GC009715.	1.0	2
107	RIFTING INITIATION THROUGH LATERAL VARIATIONS OF LITHOSPHERIC BASAL STRESS BENEATH PREEXISTING ZONES OF WEAKNESS. , 2016, , .		2
108	Lithospheric Structure underneath the Archean Tanzania Craton and Adjacent Regions from a Joint Inversion of Receiver Functions and Rayleigh-Wave Phase Velocity Dispersion. Seismological Research Letters, 2022, 93, 1753-1767.	0.8	2

STEPHEN S GAO

#	Article	IF	CITATIONS
109	A Database of Teleseismic Shear-Wave Splitting Measurements for the Ordos Block and Adjacent Areas. Seismological Research Letters, 0, , .	0.8	2
110	Mantle dynamics of the North China Craton: new insights from mantle transition zone imaging constrained by P-to-S receiver functions. Geophysical Journal International, 0, , .	1.0	2
111	Seafloor asymmetry in the Atlantic Ocean. Journal of Ocean University of China, 2004, 3, 191-194.	0.6	1
112	Highâ€accuracy practical splineâ€based 3D and 2D integral transformations in potentialâ€field geophysics. Geophysical Prospecting, 2012, 60, 1001-1016.	1.0	1
113	Seismic attributes aided fault detection and enhancement in the Sirte Basin, Libya. , 2017, , .		1
114	Prestack simultaneous inversion for delineation of the Lower Wilcox erosional remnant sandstone beneath the Texas Gulf Coastal Plain: A case study. Interpretation, 2020, 8, T991-T1005.	0.5	1
115	Crustal and Upper Mantle Structure Beneath the Southeastern United States From Joint Inversion of Receiver Functions and Rayleigh Wave Dispersion. Journal of Geophysical Research: Solid Earth, 2021, 126, e2021JB021846.	1.4	1
116	Identification of a shelf-edge submarine canyon using seismic attributes and spectral decomposition in the central Gulf Coast region of Texas. , 2018, , .		1
117	Metastable olivine within oceanic lithosphere in the uppermost lower mantle beneath the eastern United States. Geology, 0, , .	2.0	1
118	Correction to "Mantle deformation beneath southern Africaâ€: Geophysical Research Letters, 2003, 30, .	1.5	0
119	Rationale for a Permanent Seismic Network in the U.S. Central Plains Utilizing USArray. Eos, 2008, 89, 85-85.	0.1	0
120	Seismic azimuthal anisotropy and its geodynamic implications: Eastern US case study. , 2017, , .		0
121	Tectonics of the incipient continental rifting. Acta Geologica Sinica, 2019, 93, 99-100.	0.8	Ο
122	SEISMIC ANISOTROPY BENEATH THE CONTIGUOUS UNITED STATES FROM SHEAR WAVE SPLITTING ANALYSIS UTILIZING ALL THE USARRAY AND OTHER STATIONS. , 2016, , .		0
123	THE MANTLE TRANSITION ZONE BENEATH THE EAST AFRICAN RIFT SYSTEM: FROM AFAR TO OKAVANGO. , 2017,		0
124	CRUSTAL STRUCTURE AND VERTICAL MOVEMENTS OF THE UPPER MISSISSIPPI EMBAYMENT AND OZARK UPLIFT. , 2017, , .		0
125	CRUSTAL AND MANTLE STRUCTURE AND ANISOTROPY BENEATH THE YOUNG AND INCIPIENT SEGMENTS OF THE EAST AFRICAN RIFT SYSTEM. , 2017, , .		0
126	Complex seismic anisotropy beneath western Tibet and its geodynamic implications. , 2017, , .		0

#	Article	IF	CITATIONS
127	Seismic azimuthal anisotropy beneath the eastern United States and its geodynamic implications. , 2017, , \cdot		0
128	MAGMATIC DIKING AND UNDERPLATING BENEATH THE HOGGAR SWELL, ALGERIA REVEALED BY P-TO-S CONVERSIONS. , 2018, , .		0
129	CRUSTAL STRUCTURE AND SUBSIDENCE MECHANISM OF THE WILLISTON BASIN FROM RECEIVER FUNCTIONS. , 2018, , .		Ο
130	Compaction and cement volume analyses of the Lower Wilcox sandstone along the Texas Gulf Coast. , 2018, , .		0
131	Validation of poststack seismic inversion using rock-physics analysis and 3D seismic and well correlation. , 2018, , .		0
132	Hydrocarbon accumulation analysis by reconstructing the canyon-fill sequence using seismic stratigraphic interpretation in the central Gulf Coastal Plain of Texas. , 2019, , .		0
133	Pre-stack simultaneous inversion for petrophysical properties of the lower Wilcox erosional remnant sandstone along the Texas Gulf Coastal Plain. , 2019, , .		0